Inorganic Chemistry

Article

pubs.acs.org/IC

Ru(0) and Ru(II) Nitrosyl Pincer Complexes: Structure, Reactivity, and Catalytic Activity

Eran Fogler,[†] Mark A. Iron,[‡] Jing Zhang,[†] Yehoshoa Ben-David,[†] Yael Diskin−Posner,[‡] Gregory Leitus,[‡] Linda J. W. Shimon,[‡] and David Milstein*[,†]

[†]Department of Organic Chemistry and [‡]Department of Chemical Research Support, Weizmann Institute of Science, 234 Herzl Street, Rehovot 76100, Israel

Supporting Information

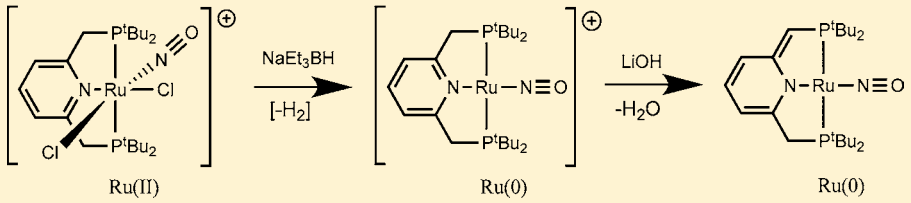

ABSTRACT: Despite considerable interest in ruthenium carbonyl pincer complexes and their substantial catalytic activity, there has been relatively little study of the isoelectronic ruthenium nitrosyl complexes. Here we describe the synthesis and reactivity of several complexes of this type as well as the catalytic activity of complex **6**. Reaction of the PNP ligand (PNP = 2,6-bis(^{t}Bu$_2$PCH$_2$)pyridine) with RuCl$_3$(NO)(PPh$_3$)$_2$ yielded the Ru(II) complex **3**. Chloride displacement by BAr^{F-} (BAr^{F-} = tetrakis(3,5-bis(trifluoromethyl)phenyl)borate) gave the crystallographicaly characterized, linear NO Ru(II) complex **4**, which upon treatment with NaBEt$_3$H yielded the Ru(0) complexes **5**. The crystallographically characterized Ru(0) square planar complex **5**·**BF$_4$** bears a linear NO ligand located trans to the pyridilic nitrogen. Further treatment of **5**·**BF$_4$** with excess LiOH gave the crystallographicaly characterized Ru(0) square planar, linear NO complex **6**. Complex **6** catalyzes the dehydrogenative coupling of alcohols to esters, reaching full conversion under air or under argon. Reaction of the PNN ligand (PNN = 2-(^{t}Bu$_2$PCH$_2$)-6-(Et$_2$NCH$_2$)pyridine) with RuCl$_3$(NO)(H$_2$O)$_2$ in ethanol gave an equilibrium mixture of isomers **7a** and **7b**. Further treatment of **7a** + **7b** with 2 equivalent of sodium isopropoxide gave the crystallographicaly characterized, bent-nitrosyl, square pyramidal Ru(II) complex **8**. Complex **8** was also synthesized by reaction of PNN with RuCl$_3$(NO)(H$_2$O)$_2$ and Et$_3$N in ethanol. Reaction of the "long arm" PN^{2}N ligand (PN^{2}N = 2-(^{t}Bu$_2$PCH$_2$−)-6-(Et$_2$NCH$_2$CH$_2$)pyridine) with RuCl$_3$(NO)(H$_2$O)$_2$ in ethanol gave complex **9**, which upon treatment with 2 equiv of sodium isopropoxide gave complex **10**. Complex **10** was also synthesized directly by reaction of PN^{2}N with RuCl$_3$(NO)(H$_2$O)$_2$ and a base in ethanol. A noteworthy aspect of these nitrosyl complexes is their preference for the Ru(0) oxidization state over Ru(II). This preference is observed with both aromatized and dearomatized pincer ligands, in contrast to the Ru(II) oxidation state which is preferred by the analogous carbonyl complexes.

INTRODUCTION

Several pyridine-based ruthenium carbonyl pincer-type complexes such as **1** and **2** (Scheme 1), developed in our laboratory,[1−3] are catalytically active in various reactions, such as the dehydrogenative coupling of alcohols to form esters (Scheme 1, eq 1),[1−4] hydrogenation of esters to alcohols (Scheme 1, eq 2),[5−7] coupling of alcohols with primary amines to form amides with liberation of H$_2$ (Scheme 1, eq 3),[8] synthesis of imines from alcohols and amines with liberation of H$_2$,[9] catalytic coupling of nitriles with amines to selectively form imines,[10] as well several other catalytic transformations.[9,11−24] It was of interest to us to explore the structure, reactivity, and catalytic activity of the isoelectronic nitrosyl complexes toward dehydrogenative coupling of alcohols to esters.

The majority of nitrosyl complexes bear a linear M−N−O group, and in such cases the NO ligand generally behaves as a 2e donor (NO$^+$). Replacing CO by an NO$^+$ ligand generates a complex with an extra positive charge, thus increasing the electrophilicity of the system, presenting a possible strategy for activation of an otherwise unreactive complex.[25,26] In cases of bent M−N−O complexes, a pair of electrons originally assigned to the metal center becomes a lone pair on nitrogen, i.e., the electron-rich metal reduces NO$^+$ to NO$^-$.[25,27,28] There are examples of complexes with both bent and linear NO ligands, and in some cases the linear and bent nitrosyl isomers are in equilibrium.[25,27,29,30] This equilibrium may provide a powerful tool for catalysis. The linear-to-bent transition effectively oxidizes the metal center by 2e and enables coordination of an additional ligand, while the bent-to-linear transition effectively reduces the complex by 2e and promotes dissociation of a ligand by stabilizing the resulting complex.[31−33] A few pincer-type ruthenium nitrosyl complexes are known in the literature, such as a Ru(II) complex, synthesized

Received: July 10, 2013
Published: September 18, 2013

dx.doi.org/10.1021/ic401780p | Inorg. Chem. 2013, 52, 11469−11479

Scheme 1. Examples of Reactions Catalyzed by Complexes 1 and 2

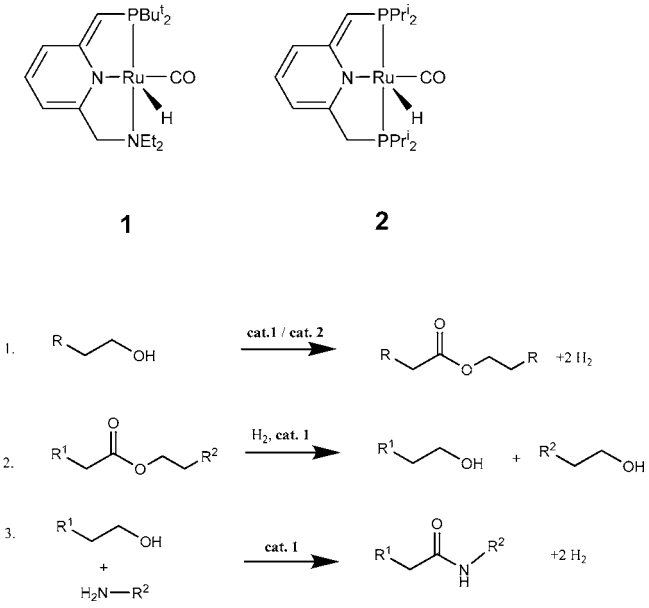

for structural studies,[34] and a Ru(0), which was prepared during research on N_2 activation.[35]

In this work, we describe the synthesis, properties, reactivity, and some catalytic activity of pyridine-based ruthenium nitrosyl pincer complexes.

RESULTS AND DISCUSSION

Synthesis and Properties of PNP–Ru Nitrosyl Complexes. Ru(II) complexes **3** and **4** were synthesized according to Scheme 2. Reaction of the PNP ligand (PNP = 2,6-bis(^{t}Bu$_2$PCH$_2$)pyridine) ligand with $RuCl_3(NO)(PPh_3)_2$ in refluxing toluene yielded complex **3**. Upon reaction of **3** with sodium tetrakis(3,5-bis(trifluoromethyl)phenyl)borate (NaBAr^F) replacement of the chloride by the BAr^F anion took place to yield complex **4** with no change in the spectroscopic data, indicating that the chloride anion in **3** was located in the outer sphere and that the structures of **3** and **4** are essentially identical. The fully characterized complexes **3** and **4** give rise to a singlet at 66.7 ppm in the $^{31}P\{^1H\}$ NMR spectrum, and the diastereotopic methylene groups of the ligand appear as a dt at 4.80 ppm (J_{HH} = 17 Hz, J_{HP} = 4.5 Hz) and a dt at 4.46 ppm (J_{HH} = 17 Hz, J_{HP} = 3.6 Hz) in the ^1H NMR spectrum. The NO stretch of **3** and **4** appears at 1867 cm^{-1} in the IR spectrum.

The entire amount of **4** was obtained as single crystals suitable for X-ray diffraction. The X-ray structure of **4** (Figure 1) reveals an octahedral structure containing two phosphorus atoms trans to each other, a chloride trans to the pyridine ligand, and a linear NO (Ru–N–O angle of 178.1°; Table 1) located trans to the second chloride. The Ru–NO bond distance of 1.775 Å is similar to the reported Ru(II)–NO bond length of 1.737 Å for an analogous pincer complex [Ru$^{(II)}$(2,2′:6′,2″-terpyridine)Cl$_2$(NO)]$^+$.[34] The Ru–P bond distances (2.444, 2.457 Å) are almost identical to the one reported for an analogous [Ru$^{(II)}$(^{t}Bu$_2$PCH$_2$SiMe$_2$)$_2$N$^-$)(NO-linear)(NO-bent)]$^+$ pincer complex (2.45(2) Å),[36] bearing a linear NO ligand trans to the amide (N$^-$) ligand.

Scheme 2. Synthesis of Complexes 3–5

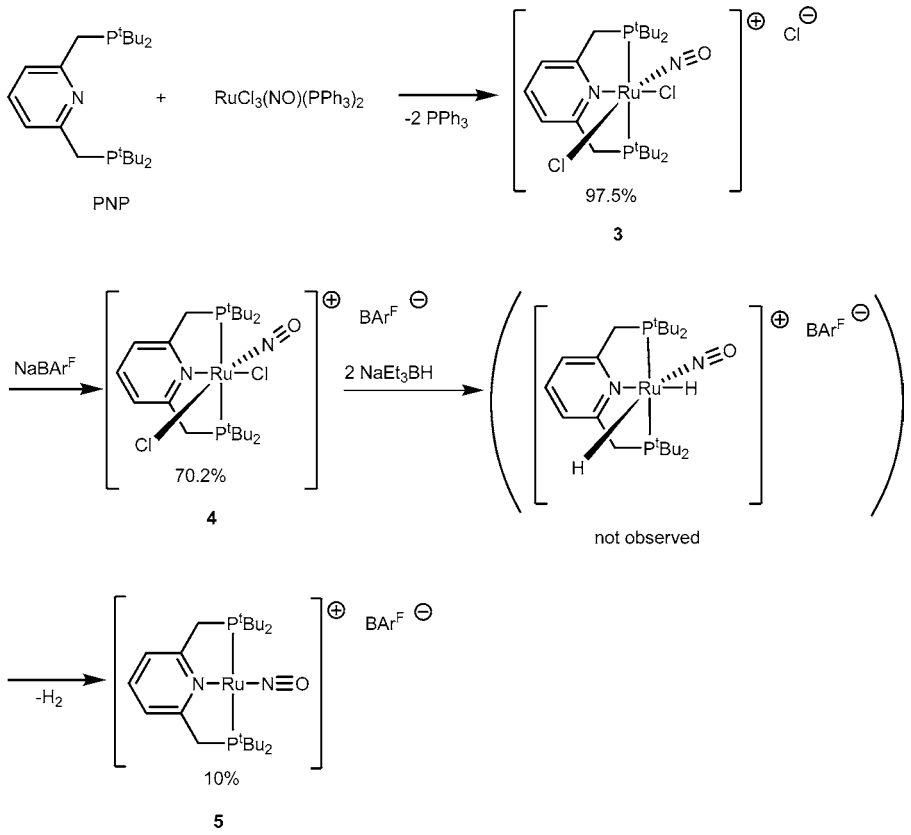

dx.doi.org/10.1021/ic401780p | Inorg. Chem. 2013, 52, 11469–11479

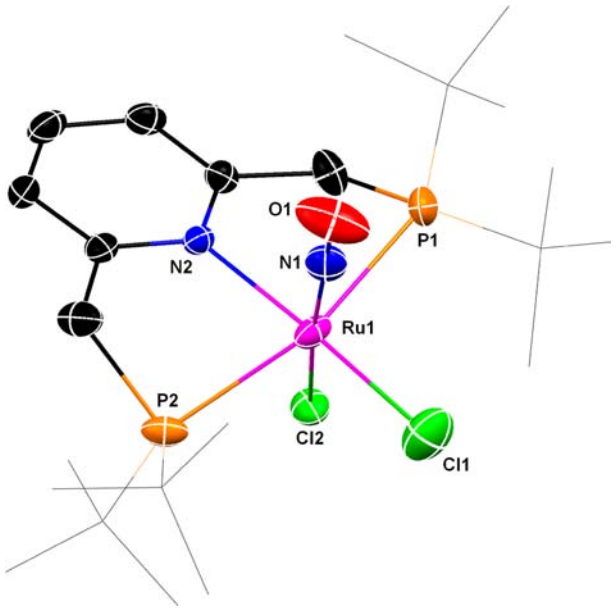

Figure 1. Structure of complex **4** (ellipsoids shown at 50% probability level). Hydrogen atoms and the BAr^F the chloride counteranion are omitted for clarity. t-Bu groups are presented as wireframe for clarity.

Table 1. Selected Bond Lengths (Å) and Bond Angles (°) in 4

Ru1−N1	1.775(7)	Ru1−Cl1	2.333(3)
N1−O1	1.123(8)	P1−Ru1−P2	163.94(2)
Ru1−P2	2.4566(7)	Ru1−N1−O1	178.1(5)
Ru1−N2	2.093(2)	N2−Ru1−N1	96.4(2)
Ru1−Cl2	2.300(2)	N2−Ru1−Cl1	172.6(3)
Ru1−P1	2.4437(7)	Cl2−Ru1−N1	172.6(2)

Complexes **3** and **4** are relatively air stable (can be exposed to air for a few minutes without decomposition); unfortunately, they slowly decompose at room temperature, resulting in some unidentified decomposition products, as observed by ^{1}H NMR. Further treatment of complex **4** with $NaBEt_3H$ in THF yielded the square planar Ru(0) complex **5**·BAr^F, which was separated and fully characterized. Complex **5** gives rise to a singlet at 80.6 ppm in the $^{31}P\{^1H\}$ NMR spectrum, and the methylene groups of the ligand appear as a triplet at 3.94 ppm (J_{PH} = 3.5 Hz) in the ^{1}H NMR spectrum. spectrum appears at 1759 cm^{-1}.

Alternatively, **5**·BF_4 was synthesized directly without the need for separation of **3**. Reaction of PNP with the Ru(II) complex $RuCl_3(NO)(H_2O)_2$ in refluxing ethanol in the presence of Et_3N under reductive conditions (ethanol is oxidized to acetone), followed by replacement of the chloride with BF_4^- using $AgBF_4$, and filtration yielded complex **5**·BF_4 as the only isolated product. Spectra of **5**·BF_4 and **5**·BAr^F are essentially identical.

Crystals of **5**·BF_4 suitable for X-ray diffraction analysis were obtained by layering pentane over a concentrated dichloromethane (DCM) solution of **5**·BF_4. The X-ray structure (Figure 2) exhibits a square planar structure containing two phosphorus atoms trans to each other and a linear NO (Ru−N−O angle of 176.4°) located trans to the pyridylic nitrogen, Table 2. The short Ru−NO bond distance of 1.708 Å indicates a stronger Ru−NO bond in the Ru(0) complex **5**·BF_4 than in Ru(II) complex **4** (1.775 Å), a result of the expected higher back-bonding in **5**·BF_4. This is also in line with the lower frequency of the NO stretch in the IR spectrum of **5**·BF_4. The reported Ru(0)−NO and Ru−P bond lengths of the analogous $Ru^{(0)}(NO)(^tBu_2PCH_2{-}SiMe_2)_2N$) pincer complex (1.721 Å and 2.380 Å, respectively)[35] are somewhat longer than those of **5**·BF_4 (1.708 and 2.349 Å, respectively). The two hydrogen atoms connected to C1 and C7A were located in the X-ray structure, indicating that **5**·BF_4 is indeed an aromatic complex.

The ruthenium nitrosyl complex **5** adopts the aromatic PNP−Ru(0) structure rather then the unobserved dearomatized-PNP* Ru(II) hydride form **5′** (Figure 3), unlike the analogous carbonyl complexes **1** and **2**.

The aromatic structure of **5**·BF_4 is clearly evident in its crystal structure, in which the two hydrogen atoms connected to C1 and C7A were located. In addition, the pairs of bonds C1−C2/C6−C7A, C2−C3/C5−C6, C3−C4/C4−C5, and N1−C2/N1−C6 are (within experimental error) of the same length, unlike the expected alternating bond lengths in the putative Ru(II) dearomatized complex **5′**.

Attempts to synthesize the dearomatized Ru(0) complex **6** by deprotonation of **5**·BF_4 with KOtBu (potassium *tert*-butoxide) or KHMDS (potassium bis-hexamethyldisilazide) led to decomposition of the complex. However, when **5**·BF_4 was reacted with a suspension of LiOH (large excess) in THF, complex **6** was obtained as the sole product (Scheme 4).

Complex **6** gives rise to two doublets in the $^{31}P\{^1H\}$NMR spectrum at 78.73 and 74.88 ppm (J_{PP} = 200 Hz). In the ^{1}H NMR spectrum, the methylene groups of the ligand appear as a doublet at 2.81 ppm (J_{PH} = 8.7 Hz) and the "arm" vinylic proton appears as a doublet (J_{HP} = 3.6 Hz) at 3.81 ppm. The corresponding carbon exhibits a doublet at 67.8 ppm (J_{CP} = 49.0 Hz) in the $^{13}C\{^1H\}$ NMR spectrum. The NO stretches in the IR spectrum appear at 1916 cm^{-1}. Single crystals of **6** suitable for X-ray diffraction were obtained by slow evaporation of its etheral solution.

The X-ray structure of **6** (Figure 4) reveals a square planar geometry with the two phosphorus atoms located trans to each other and a linear nitrosyl group (Ru−N−O angle of 179.6°) located trans to the dearomatized pyridine nitrogen, indicating that **6** is a Ru(0) complex. Comparing the Ru(0)−NO bond

Scheme 3. Synthesis of 5·BF_4

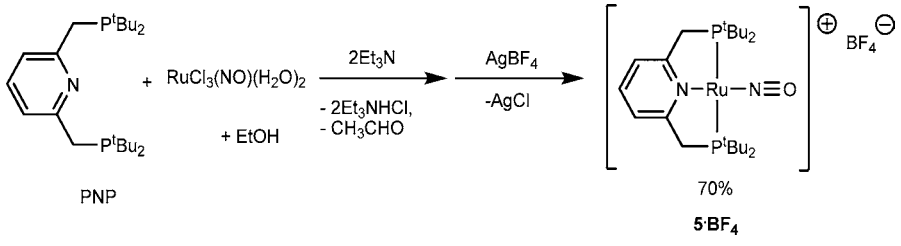

dx.doi.org/10.1021/ic401780p | *Inorg. Chem.* 2013, 52, 11469−11479

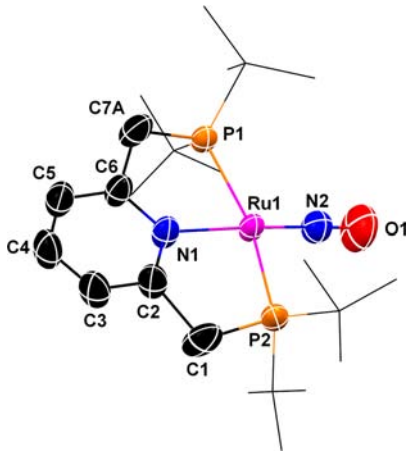

Figure 2. X-ray structure of complex **5**·BF_4 (ellipsoids shown at 50% probability level). Hydrogen atoms and counteranion are omitted for clarity. t-Bu groups are presented as wireframe for clarity.

Table 2. Selected Bond Lengths (Å) and Bond Angles (°) in 5·BF_4

Ru1−N2	1.708(4)	C5−C6	1.366(7)
N2−O1	1.157(6)	C3−C4	1.359(8)
Ru1−P1	2.349(1)	C4−C5	1.360(8)
Ru1−P2	2.349(1)	N1−C2	1.362(6)
Ru1−N1	2.139(4)	N1−C6	1.358(6)
C1−C2	1.511(7)	Ru1−N2−O1	176.4(5)
C6−C7A	1.48(1)	P2−Ru1−P1	165.24(5)
C2−C3	1.368(7)	N1−Ru1−N2	174.8(2)

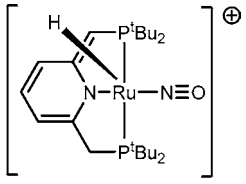

5'

Figure 3. Unobserved dearomatized complex **5**′.

Scheme 4. Synthesis of 6

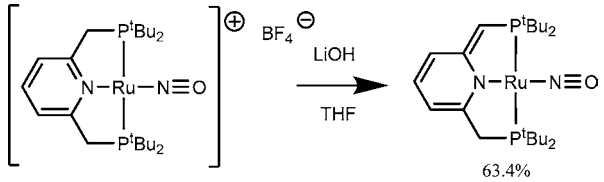

5·BF_4 **6**

lengths of **6** and **5**·BF_4 shows a slightly longer Ru−NO in **6** (1.721 vs 1.708 Å) and a slightly longer N−O bond length (1.175 vs 1.157 Å), Table 3. The difference in P1−C1 (1.779 Å) and P2−C7 (1.817 Å) indicates the contribution of a partial P1═C1 double bond to the resonance structure of complex **6**.

Next, we explored the reactivity of **6** with water and methanol. The NMR spectrum of complex **6** in a solution of toluene saturated with water or in THF containing 10−15% water (**6** is insoluble in water, and adding more than 15% water to a THF solution of **6** resulted in phase separation) was identical to the spectrum of **6** in the absence of water, even upon heating the THF/water solution to 50 °C for 14 h.

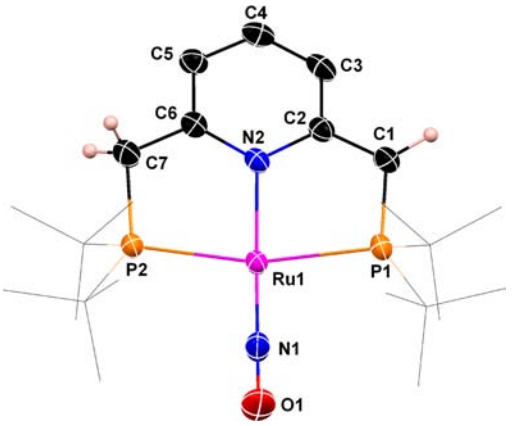

Figure 4. X-ray structure of complex **6** (ellipsoids shown at 50% probability level). Hydrogen atoms (except for the methylene and vinylic protons) are omitted for clarity. t-Bu groups are presented as wireframe for clarity.

Table 3. Selected Bond Lengths (Å) and Bond Angles (°) in 6

Ru1−N1	1.721(3)	C2−C3	1.423(5)
N1−O1	1.175(4)	C5−C6	1.389(4)
Ru1−P1	2.3537(10)	C3−C4	1.371(5)
Ru1−P2	2.3452(9)	C4−C5	1.398(5)
Ru1−N2	2.098(3)	Ru1−N1−O1	179.6(4)
C1−C2	1.410(5)	P1−Ru1−P2	164.44(3)
C6−C7	1.463(5)	N2−Ru1−N1	178.3(1)
P1−C1	1.779(4)	P1−C1−C2	116.4(3)
P2−C7	1.817(3)	C6−C7−P2	114.5(3)

However, when **6** was dissolved in dry methanol, it underwent protonation to give **5** (and presumably methoxide as the counteranion) as the only product as observed by $^{31}P\{^1H\}$ NMR as a result of the large excess of the methanol solvent (Scheme 5). This reaction is fully reversible and upon evaporation of the methanol solvent **6** was formed. This cycle can be repeated several times.

According to DFT calculations, **5**′, the dearomatized isomer of **5**, is much less stable than **5** ($\Delta\Delta G_{298}$ = 30.0 kcal/mol). For comparison, the CO analogue of **5**′, the putative complex **2**′, is slightly less stable than the dearomatized complex **2a** (**2** with P^{t}Bu$_2$), $\Delta\Delta G_{298}$ = 2.2 kcal/mol, Scheme 6.

The likely explanation for this large difference in stability between **5** and **5**′ is the lower electron density at the metal center in the nitrosyl complexes as compared with the corresponding carbonyl complexes. This is indicated by the more positive atomic polar tensor (APT) charges on the ruthenium centers of the various complexes (Table 4). Comparing complexes **2a** and **5** (both with the PNP ligand), the partial atomic charge on the ruthenium center is more

Scheme 5. Protonation of 6 in MeOH Solution

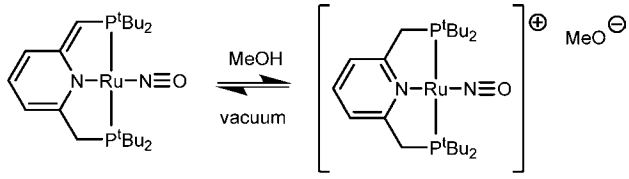

6 **5**

dx.doi.org/10.1021/ic401780p | *Inorg. Chem.* 2013, 52, 11469−11479

Scheme 6. Free Energy Difference between 5 and 5′ and between 2 and 2′

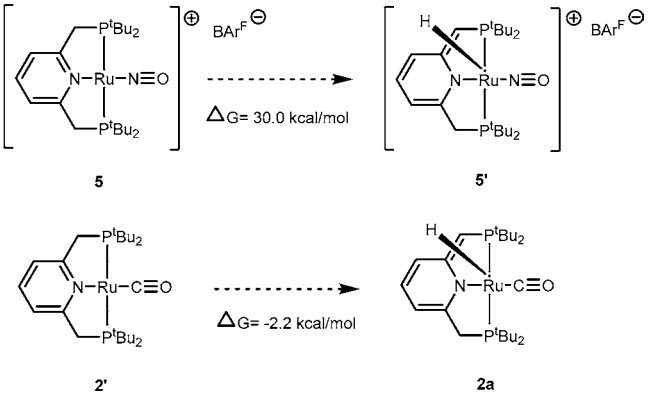

Table 4. DFT Partial (APT) Charges on Ru

		APT charge	
complex	L	aromatic ligand	dearomatized
1 (PNN ligand)	CO	−0.24	0.25
2a	CO	−1.21 (**2′**)	−0.54 (**2a**)
5	NO	−0.56 (**5**)	0.16 (**5′**)
6	NO		−0.49

positive in the NO complex than in the CO complex; in fact, the charge on the metal in the dearomatized CO complex **2a** (−0.54) is similar to the charge in the aromatized NO complex **5** (−0.56). This is caused by the fact that the nitrosyl complex is positively charged, and the nitrosyl ligand is a stronger π acceptor. It is also notable that in the dearomatized Ru(0) NO complex **6** the charge on Ru is similar to that in the Ru(II) **2a** and the cationic Ru(0) **5**.

Synthesis and Properties of PNN Nitrosyl Complexes. Reaction of the PNN ligand (PNN = 2-(^{t}Bu$_2$PCH$_2$)-6-(Et$_2$NCH$_2$)pyridine) with RuCl$_3$(NO)(H$_2$O)$_2$ in ethanol followed by solvent evaporation led to a solid which is likely a mixture of isomers **7a** and **7b** (Scheme 7). It exhibits two singlets at 97.0 and 86.8 ppm in CD$_2$Cl$_2$ (integration ratio of 0.4:1) or two singlets at 96.2 and 87.0 ppm in EtOH (integration ratio of 0.24:1) in the ^{31}P{^{1}H}NMR spectrum. The methylene groups of the phosphorus arm of the ligand appear as multiplets at 3.32 and 3.63 ppm for **7a** and at 3.45 ppm for **7b** (see Experimental Section) in the ^{1}H NMR spectrum (diastereotopic methylenes for **7a** and nondiastereotopic methylenes for **7b** are consistent with the symmetry across the meridional pincer plane). The NO stretches in the IR spectrum appear at 1855 and 1826 cm^{-1}. The postulated isomers, **7a** and **7b**, are probably in equilibrium. Thus, the ratio of the peaks in the ^{31}P{^{1}H}NMR spectrum changed after evaporation and replacement of the DCM solvent with EtOH. A second evaporation of the EtOH and addition of the original solvent (DCM) restored the original ratio between **7a** and **7b**. In addition, in order to eliminate the possibility that outer-sphere chloride is taking part in the equilibrium, we replaced the chloride anion with the BAr^F anion, resulting in no change in the spectra of **7a** and **7b** (but it increased their solubility in ether).

The geometries of isomers **7a** and **7b** were optimized using DFT. The energies in ethanol and benzene for each of the complexes, relative to the most stable complex, are listed in Table 5. In benzene, the energy difference between **7a** and **7b** is very small (0.09 kcal/mol in favor of **7b**). In ethanol, the energy difference is 2.19 kcal/mol in favor of **7a**. Therefore, an equilibrium between **7a** and **7b**, as suggested by the experimental results, is likely.

Reaction of the mixture of **7a** + **7b** with 2 equiv of sodium isopropoxide gave the bent nitrosyl complex **8**. Interestingly, when the reaction was performed in a closed system **8** was not obtained; hence, it is possible that liberation of H$_2$ drives the reaction. Perhaps substitution of the chlorides by isopropoxide followed by β-H elimination yields a dihydride intermediate which slowly loses H$_2$ (3 days in refluxing ether) to give a Ru(0) complex analogous to **5** which reacts with chloride to give the Ru(II) complex **8**, Scheme 8.

Complex **8** gives rise to a singlet at 56.6 ppm in the ^{31}P{^{1}H}NMR spectrum, and the phosphine methylene groups of the ligand appear as a doublet at 3.27 ppm (J_{PH} = 11 Hz) in the ^{1}H NMR spectrum (C_s symmetry for **8** was observed in the ^{1}H NMR due to fast conformational change; for more details see DFT calculations below). The NO stretches in the IR spectrum of the solid (NaCl plate) appear at 1928 and 1679 cm^{-1}, indicating the presence of both bent and linear NO in the solid state (see DFT Calculations below).

Crystals of **8** suitable for X-ray diffraction analysis were obtained by slow evaporation of ethanol from a concentrated ethanol solution of **8**. The X-ray structure (Figure 5 and Table 6) exhibits a square pyramidal structure with the phosphine ligand located trans to the tertiary amine, a bent NO (Ru−N−O angle of 130.2°) located cis to the pyridine-based ligand, and an equatorial chloride.

Distances and angles in **8** are similar to those of related square pyramidal pincer Ru(II) nitrosyl complexes such as [Ru$^{(II)}$(^{t}Bu$_2$PCH$_2$SiMe$_2$)$_2$N)(NO-linear)(NO-bent)]$^+$.[36] The Ru−NO bond distance is 1.837 Å, somewhat shorter than

Scheme 7. Synthesis of Complex 7

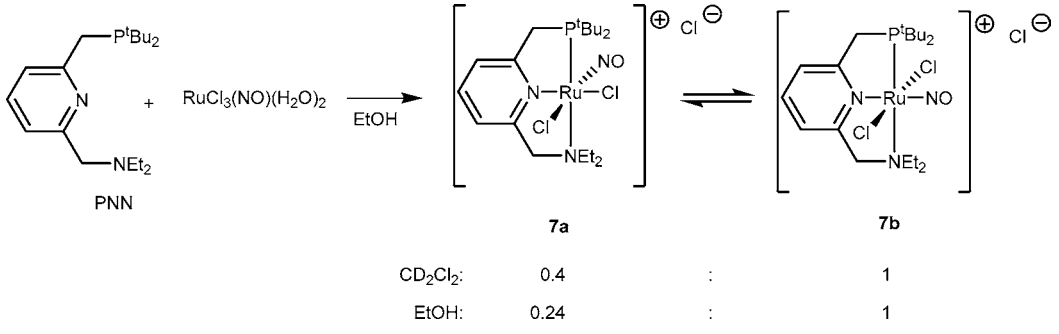

dx.doi.org/10.1021/ic401780p | Inorg. Chem. 2013, 52, 11469−11479

Table 5. Relative Energies (kcal/mol) of Isomers 7a and 7b

	$\Delta G_{298,\ EtOH}$	$\Delta G_{298,\ C6H6}$
7a	0.00	0.09
7b	2.19	0.00

Scheme 8. Synthesis of Complex 8

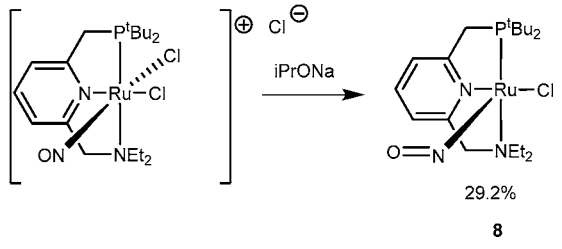

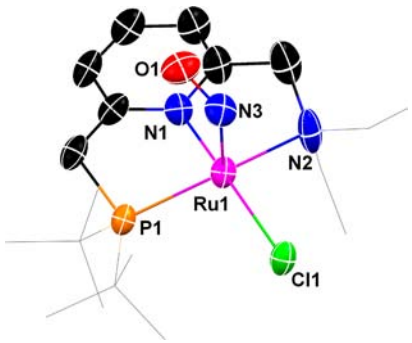

Figure 5. Structure of complex **8** (ellipsoids shown at 50% probability level). Hydrogen atoms and counteranion are omitted for clarity. t-Bu and Et groups are presented as wireframe for clarity.

Table 6. Selected Bond Lengths (Angstroms) and Bond Angles (degrees) of 8

Ru1–N3	1.837(5)	Ru1–Cl1	2.420(2)
N3–O1	1.207(7)	Ru1–N3–O1	130.2(4)
Ru1–P1	2.265(2)	P1–Ru1–N2	150.8(1)
Ru1–N1	2.033(5)	N1–Ru1–Cl1	168.9(1)
Ru1–N2	2.269(5)	N1–Ru1–N3	90.0(2)

the reported Ru(II)–(bent NO) bond length of 1.910 Å for the analogous pincer complex $[Ru^{(II)}(^tBu_2PCH_2SiMe_2)_2N^-)(NO\text{-linear})(NO\text{-bent})]^+$. The Ru–Cl bond is longer in **8** (2.420 Å) than in **4** (2.300 and 2.333 Å), probably due to fast conformational changes. DFT calculations on **8** indicate two square pyramidal isomers, one with a bent NO in the apical position (**8**) and another with a linear NO in the equatorial position (**8′**) (Scheme 9). These isomers are very close in energy; in both ethanol and benzene **8′** is slightly more stable by $\Delta G_{298,sol} = -1.5$ kcal/mol.

These calculations are supported by the fact that according to IR spectroscopy both linear and bent NO complexes are present in the solid state (1928 cm^{-1} and 1679 cm^{-1}), although only one compound is observed in solution.

Complex **8** can also be synthesized by a simpler route involving $RuCl_3(NO)(H_2O)_2$ and PNN in refluxing ethanol to form **7** in situ, which is further reduced to **8** by EtOH and Et_3N, (Scheme 10).

Synthesis and Properties of PN^{2}N Nitrosyl Complexes. Next, we set out to prepare complexes of the "long arm" PNN ligand: PN^{2}N (2-(^{t}Bu$_2$PCH$_2$)-6-(Me$_2$NCH$_2$CH$_2$)pyridine). First, we synthesized the Ru(II) dichloride complex **9** by complexation of PN^{2}N with $RuCl_3(NO)(H_2O)_2$ (Scheme 11).

The fully characterized complex **9** gives rise to a singlet at 94.3 ppm in the $^{31}P\{^1H\}$NMR spectrum, and the phosphorus methylene groups of the ligand appear as a double doublet at 5.03 and 4.29 ppm (J_{HH} = 17.1 Hz, J_{HP} = 10.2 Hz) in the ^1H NMR spectrum. The NO stretch in the IR spectrum appears at 1855 cm^{-1}.

Crystals suitable for X-ray analysis were obtained by slow evaporation of a concentrated CH_2Cl_2 solution of **9**. The X-ray structure of **9** (Figure 6) exhibits an octahedral structure containing phosphorus atoms trans to the tertiary amine, a chloride trans to the pyridine ligand, and a linear NO (Ru–N–O angle of 175.4°) trans to chloride. Bond lengths and angles of **9** are similar to those of **4** (Table 7).

Comparing **9** to **4**, the Ru(II)–NO bond length of **9** (1.744 Å) is shorter than that of **4** (1.775 Å) and the N–O distance in **9** (1.150 Å) is longer then in **4** (1.123 Å). This indicates more back-donation to the NO ligand of **9**. In addition, all Ru–ligand distances are longer in **9** in comparison to **4**.

Ru complex **10** was synthesized in two ways, as outlined in Scheme 12: (a) reaction of complex **9** with NaO^{i}Pr as a hydride source (by β-H elimination after chloride substitution followed by elimination) resulted in 30% yield and (b) by tandem reaction in refluxing ethanol in which **9** was formed in situ, resulting in higher yield (87%).

The fully characterized complex **10** gives rise to a singlet at 56.9 ppm in the $^{31}P\{^1H\}$NMR spectrum, and the phosphorus methylene groups of the ligand appear as a doublet at 3.24 ppm (J_{HP} = 10.8 Hz) in the ^1H NMR spectrum (the reason we can see C_s symmetry for **10** in the ^1H NMR is probably due to fast conformational change similar to **8**). spectrum appears at 1589 cm^{-1}, as expected for bent NO.

Dehydrogenative Coupling of Alcohols to Esters Catalyzed by 6. Catalytic dehydrogenative coupling of alcohols to esters is of central interest in organic synthesis. The PNP and PNN pyridine-based ruthenium pincer complexes **1** and **2** catalyze dehydrogenative coupling of alcohols to esters and H_2 (Scheme 1, eq 1).[1–3] Similarly, an acridine-based PNP ruthenium carbonyl pincer-type complex developed in our laboratory catalyzes (in the presence of base) conversion of alcohols to esters and H_2.[11] We now find that complex **6** catalyzes this reaction as well. The reaction can be

Scheme 9. Complexes 8 and 8′

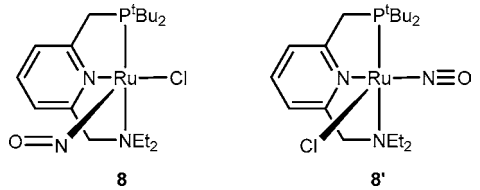

Scheme 10. Alternative Synthesis of Complex 8

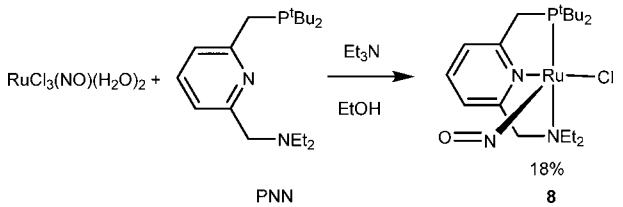

dx.doi.org/10.1021/ic401780p | Inorg. Chem. 2013, 52, 11469–11479

Scheme 11. Synthesis of Complex 9

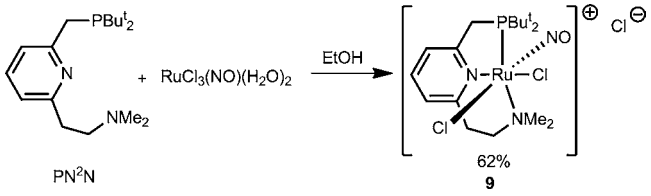

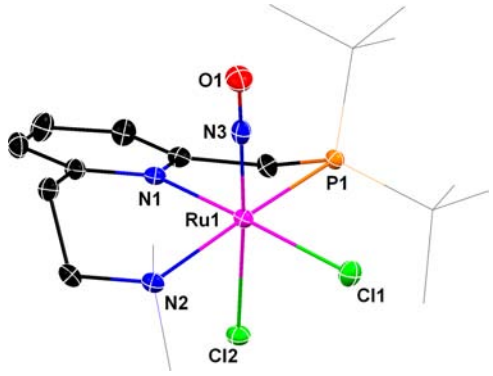

Figure 6. Structure of complex **9** (ellipsoids shown at 50% probability level). Hydrogen atoms and counteranion are omitted for clarity. t-Bu and Me groups are presented as wireframe for clarity.

Table 7. Selected Bond Lengths (Å) and Bond Angles (°) in 9

Ru1–N3	1.744(2)	Ru1–Cl2	2.3313(6)
N3–O1	1.150(3)	Ru1–N3–O1	175.4(2)
Ru1–P1	2.3940(7)	P1–Ru1–N2	174.46(6)
Ru1–N1	2.130(2)	N3–Ru1–N1	95.9(1)
Ru1–N2	2.268(2)	N1–Ru1–Cl1	173.67(6)
Ru1–Cl1	2.3877(7)	N3–Ru1–Cl2	176.29(7)

Scheme 12. Two Synthetic Routes to Complex 10

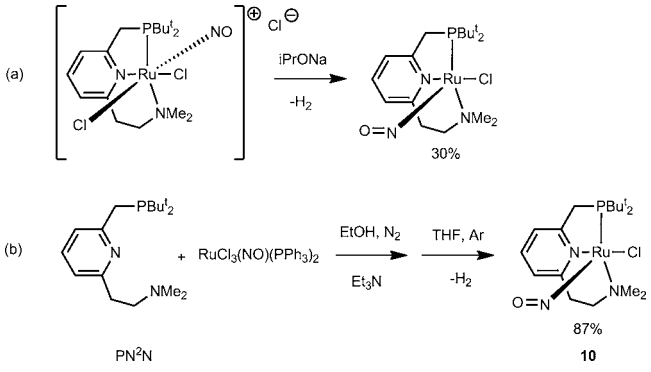

carried out under air, reaching full conversion and quantitative yield after 12 h. Hexanol was chosen as a typical substrate (Scheme 13).

Attempts to catalyze similar reactions under the same conditions using other complexes described in this work gave disappointing results (for example, **8** gave 15% conversion of hexanol to the corresponding acetal (1,1-bis(hexyloxy)hexane) after 26 h). Therefore, we decided to suspend the inquiry of the catalytic activity of these complexes for the present time.

CONCLUSION

We synthesized and characterized the ruthenium nitrosyl aromatic complexes **3**, **4**, **5**, **7**, **8**, **9**, and **10** and the dearomatized ruthenium nitrosyl complex **6**. We found that complex **6** catalyzes the dehydrogenative coupling of hexanol to form hexyl hexanoate, reaching full conversion under either air or argon. The nitrosyl complexes adopt the Ru(0) rather than the Ru(II) oxidization state, in contrast to their carbonyl analogs. This preference was observed with both aromatized and dearomatized pincer ligands. DFT calculations show that the partial charge on the Ru(0) of the nitrosyl complexes is similar to their Ru(II) carbonyl analogs, suggesting that the electron density at the metal center plays a major role in determining the aromatic nature of the ligand and the overall structure of the complex.

EXPERIMENTAL SECTION

General Procedures. All experiments with metal complexes and phosphine ligands were carried out under an atmosphere of purified nitrogen in a Vacuum Atmospheres glovebox equipped with a MO 40-2 inert gas purifier or using standard Schlenk techniques. All solvents were reagent grade or better. All nondeuterated solvents were refluxed over sodium/benzophenone ketyl and distilled under argon atmosphere. Deuterated solvents were used as received. All solvents were degassed with argon and kept in the glovebox over 4 Å molecular sieves. Commercially available reagents were used as received. $RuCl_3(NO)(PPh_3)_2$[37] was prepared according to a literature procedure.^{1}H, ^{13}C, and ^{31}P spectra were recorded at 400, 100,162, and 376 MHz using Bruker AMX-300, AMX-400, and AMX-500 spectrometers. All spectra were recorded at 295 K unless otherwise noted. ^{1}H NMR and ^{13}C{^{1}H} NMR chemical shifts are reported in ppm downfield from tetramethylsilane and referenced to the residual signals of an appropriate deuterated solvent. ^{31}P NMR chemical shifts are reported in ppm downfield from H_3PO_4 and referenced to an external 85% solution of phosphoric acid in D_2O. ESI-MS spectroscopy was performed by the Department of Chemical Research Support, Weizmann Institute of Science. The nitrosyl complexes described in this work were unstable toward light and air, and all reactions were performed in the dark. Accurate elemental analysis could not be obtained (elemental analysis results were not reproducible even when single crystals (of **4**) were used from the same batch). HRMS was determined.

Scheme 13. Dehydrogenative Coupling of Hexanol to Hexyl Hexanoate Catalyzed by 6

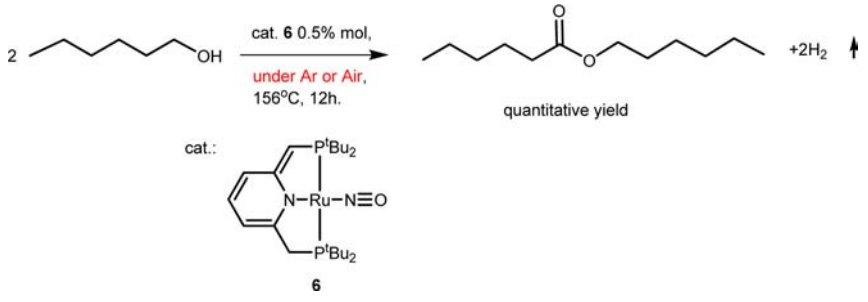

dx.doi.org/10.1021/ic401780p | Inorg. Chem. 2013, 52, 11469–11479

Synthesis of 3. To a 10 mL flask equipped with a gas inlet were added $RuCl_3(NO)(PPh_3)_2$ (20 mg, 0.026 mmol), ^{t}Bu-PNP (10.3 mg, 0.026 mmol), and toluene (1 mL) under nitrogen atmosphere. The reaction mixture was stirred under reflux overnight, resulting in red crystals of **3**. The reaction mixture was allowed to cool to ambient temperature and filtered. Crystals were rinsed with toluene (2 mL) and pentane (2 mL) and dried under vacuum to give complex **3** as a red solid in 97% yield. $^{31}P\{^1H\}$ NMR (CD_2Cl_2): 66.7 (**s**). ^1H NMR (CD_2Cl_2): 8.18 (d, $^3J_{HH}$ = 7.8 Hz, 2H, Py-H3, H5), 8.09 (t, 1H, $^3J_{HH}$ = 7.8 Hz, Py-H4), 4.80 (dt, $^2J_{HH}$ = 17 Hz, $^2J_{HP}$ = 4.5 Hz, 2H, PC*H*HPy), 4.46 (dt, $^2J_{HH}$ = 17 Hz, $^2J_{HP}$ = 3.6 Hz, 2H, PC*H*HPy), 1.60 (d, $^3J_{HP}$ = 7.2 Hz, 18H, $PC(CH_3)_3$, 1.55 (d, $^3J_{HP}$ = 7.2 Hz, 18H, $PC(CH_3)_3$. $^{13}C\{^1H\}$ NMR (CD_2Cl_2): 164.1 (s, Py-C2, C6) 142.9 (s, Py-C4), 125.4 (s, Py-C3, C5), 42.1 (t, $^1J_{CP}$ = 2.2 Hz, $PC(CH_3)_3$), 41.3 (t, $^1J_{CP}$ = 6.7 Hz, $PC(CH_3)_3$), 38.0 (t, $^1J_{CP}$ = 8.7 Hz, PCH_2Py), 30.7 (bm, $PC(CH_3)_3$). IR: ν N−O 1867 cm^{-1}. HRMS: *m*/*z* 597.1295 (M^+, calcd *m*/*z* 597.1271).

Synthesis of 4. To an ethereal suspension (4 mL) of **3** (20 mg, 0.0316 mmol) was added 1 equiv of $NaBAr^F$ (28 mg, 0.0316 mmol) under nitrogen atmosphere. The reaction mixture was stirred for 2 h at room temperature for reaction completion, and then the NaCl was filtered off, and the solvent was slowly removed under vacuum, giving a red crystal of **4**, suitable for X-ray analysis in 70% yield. HRMS: *m*/*z* 597.1272 (M^+, calcd *m*/*z* 597.1271). The rest of the spectra are identical those of **3**.

Reaction of 4 with $NaBEt_3H$ to yield 5·BAr^F. To a solution of **4** (36.5 mg, 0.025 mmol) in THF (5 mL) was added $NaBEt_3H$ (56 μL, ∼1 M solution, 0.05 mmol) under a nitrogen atmosphere at room temperature. The reaction mixture was stirred for 110 min, after which the solvent was removed under vacuum and the residue was left under vacuum for 2 h. The residue was extracted with pentane, and pentane was removed under vacuum to yield pure **5** as a green solid in 10% yield.

For clarity, signals of BAr^F are omitted from ^1H and $^{13}C\{^1H\}$ NMR. $^{31}P\{^1H\}$ NMR (CD_2Cl_2): 80.6(s). ^1H NMR (CD_2Cl_2): 7.79 (t, 1H, $^3J_{HH}$ = 7.5 Hz, Py-H4), 7.47 (d, 2H, $^3J_{HH}$ = 7.5 Hz, Py-H3, H5), 3.94 (t, 4H, $^2J_{PH}$ = 3.5 Hz, Py-CH_2P), 1.53 (t, 36H, $^2J_{PH}$ = 7.5 Hz, $P(C(CH_3)_3)_2$). $^{13}C\{^1H\}$ NMR (CD_2Cl_2): 167.1 (t, J_{PC} = 6.9 Hz, Py-C2, C6), 142.5 (s, Py-C4), 122.6 (t, J_{PC} = 5.0 Hz, Py-C3, C5), 37.6 (t, J_{PC} = 8.8 Hz, $P(C(CH_3)_3)_2$), 34.8 (t, J_{PC} = 8.8 Hz, $PyCH_2P$), 29.9 (t, J_{PC} = 2.7 Hz, $P(C(CH_3)_3)_2$). IR: ν N−O 1759 cm^{-1}. HRMS: *m*/*z* 527.1901 (M^+, calcd *m*/*z* 527.1894).

Synthesis of 5·BF_4. To a solution of $Ru(NO)Cl_3{\cdot}2H_2O$ (26 mg, 0.1 mmol) in ethanol (10 mL) was added t-Bu-PNP (40 mg, 0.1 mmol) and NEt_3 (30.3 mg, 0.3 mmol), and the mixture was heated at 78 °C for 4 h. Upon cooling to room temperature, the red-purple solution was taken to dryness under vacuum and the residue was extracted with THF (3 × 5 mL). To the combined THF solution was added $AgBF_4$ (19.5 mg, 0.1 mmol); the mixture was stirred in the dark for 0.5 h and then filtered. The filtrate was concentrated to 2 mL, and then 10 mL of diethyl ether was added slowly to precipitate a brown-red solid of **5**·BF_4 (43 mg, 70%). Spectra of **5**·BF_4 are identical to those of **5**·BAr^F, except for the signals associated with BAr^F.

Synthesis of 6. To a solution of **5**·BF_4 (125 mg, 0.267 mmol) in THF (4 mL) was added LiOH (125 mg, 5.22 mmol) under nitrogen atmosphere at room temperature. The suspended reaction mixture was stirred for 1 h and 30 min, after which the solvent was removed under vacuum. The residue was extracted with pentane (3 × 5 mL), and the solvent was removed under vacuum to yield pure **6** as a black/blue solid in 63% yield. Single crystals of **6** suitable for X-ray diffraction were obtained by slow evaporation of an etheral solution. $^{31}P\{^1H\}$ NMR (C_6D_6): 78.7 (d, 1P, $^2J_{PP}$ = 200 Hz), 74.9 (d, 1P, $^2J_{PP}$ = 200 Hz). ^1H NMR (C_6D_6): 6.06 (bd, 2H, Py-H3 + H5), 5.03 (m, 1H, Py-H5), 3.81 (d, $^2J_{H,P}$ = 3.6 Hz, 1H, PyC*H*P), 2.81 (d, $^2J_{HP}$ = 8.7 Hz, 2H, PCH_2Py), 1.63 (d, 18H, $^3J_{PH}$ = 12.6 Hz, $P(C(CH_3)_3)_2$), 1.27 (d, 18H, $^3J_{PH}$ = 12.6 Hz, $P(C(CH_3)_3)_2$). $^{13}C\{^1H\}$ NMR (toluene-d_8): 173.2 (d, $^2J_{CP}$ = 21.4, 5 Hz, Py-C2), 160.8 (m, Py-C6) 131.7 (s, Py-C4), 116.4 (d, $^3J_{CP}$ = 18.8 Py-C3), 98.4 (d, $^3J_{CP}$ = 11.3 Py-C5), 67.8 (d, $^1J_{CP}$ = 49.0, PyCHP), 37.4 (d, $^1J_{CP}$ = 22.6, $PyCH_2P$), 36.2 (d, $^1J_{CP}$ = 15.1 Hz, $P(C(CH_3)_3)_2$), 33.1 (d, $^1J_{CP}$ = 16.3 Hz, $P(C(CH_3)_3)_2$), 30.2 (d, $^2J_{CP}$ = 5 Hz, $P(C(CH_3)_3)_2$), 29.6 (d, $^2J_{CP}$ = 5 Hz, $P(C(CH_3)_3)_2$). IR: ν N−O 1916.0 cm^{-1}. HRMS: *m*/*z* 527.1909 ($(M + H)^+$, calcd *m*/*z* 527.1894).

Reversible Protonation of 6 with Methanol (Scheme 5). Analytically pure **6** (8.6 mg, 0.01636 mmol) was dissolved in MeOH (1 mL) under nitrogen atmosphere at room temperature. $^{31}P\{^1H\}$ NMR was taken showing only one peak, at 80.6 ppm, indicating formation of the cationic complex **5** (presumably with methoxide counteranion). Solvent was removed under vacuum, and the residue was dissolved in C_6D_6, resulting in full restoration to the starting material **6** as indicated by NMR. This procedure was repeated three times using the same sample of **6**.

Synthesis of 7. To a solution of $RuCl_3(NO)(H_2O)_2$ (100 mg, 0.366 mmol) in ethanol (5 mL) was added PNN (118 mg, 0.366 mmol) under nitrogen atmosphere. The reaction mixture was stirred for 5 h at room temperature, after which the solvent was removed under vacuum, the residue was extracted with 5 mL of CH_2Cl_2 and centrifuged, and the CH_2Cl_2 solution was filtered and concentrated to 1 mL. Addition of pentane resulted in precipitation of pure **7** in 68% yield. $^{31}P\{^1H\}$ NMR (CD_2Cl_2): 97.0 (s, 0.4P, a), 86.8 (s, 1P, b). $^{31}P\{^1H\}$ NMR (EtOH): 96.2 (s, 0.24P, a), 87.0 (s, 1P, b). Two peaks are observed due to isomers **7a** and **7b**. ^1H NMR (CD_2Cl_2): 8.30 (m, 1H, Py-H4 a + b,), 8.1 (bs, 1H, Py-H5 a + b), 7.77 (m, 1H, Py-H3 a + b), 5.01 (bm, 1H, NC*H*HPy a), 4.78 (bm, 2H, NCH_2Py b), 4.67 (bm, 1H, NC*H*HPy a), 3.63 (m, 1H, PyC*H*HP a), 3.45 (m, 2H, $PyCH_2P$ b), 3.32 (m, 1H, PyC*H*HP a), 1.59 (bm, 18H, $P(C(CH_3)_3)_2$ a + b), 1.44 (bm, 2H, $N(CH_2CH_3)_2$ a + b), 1.25 (bm, 3H, $N(CH_2CH_3)_2$). $^{13}C\{^1H\}$ NMR (CD_2Cl_2): 162.5 (s, Py-C2 A), 162.2 (s, Py-C2 B) 159.7 (s, Py-C6 A), 159.5 (s, Py-C6 B), 143.3 (s, Py-C4 B), 142.7 (s, Py-C4 A), 125.8 (d, $^3J_{CP}$ = 8 Hz, Py-C3 A), 125.6 (d, $^3J_{CP}$ = 10 Hz, Py-C3 B), 123.3 (s, Py-C5 A), 122.9 (s, Py-C5 B), 67.8 (s, $PyCH_2N$ A), 64.2 (s, $PyCH_2N$ B), 50.5 (s, $N(CH_2CH_3)(CH_2CH_3)$, A), 48.5 (s, $N(CH_2CH_3)(CH_2CH_3)$, A), 47.7 (s, $N(CH_2CH_3)_2$), B), 43.0 (d, $^1J_{CP}$ = 14.9 Hz, $P(C(CH_3)_3)(C(CH_3)_3)$ A), 42.0 (d, $^1J_{CP}$ = 14.9 Hz, $P(C(CH_3)_3)(C(CH_3)_3)$ A), 41.4 (d, $^1J_{CP}$ = 12.7 Hz, $P(C(CH_3)_3)_2$ B), 38.3 (d, $^1J_{CP}$ = 23.3 Hz, $PyCH_2P$ A), 37.2 (d, $^1J_{CP}$ = 24.6 Hz, $PyCH_2P$ B), 31.0 (bs, $P(C(CH_3)_3)_2$ B) 30.1 (s, $P(C(CH_3)_3)$ $(C(CH_3)_3)$ A), 30.0 (s, $P(C(CH_3)_3)(C(CH_3)_3)$ A), 10.6 (s, $N(CH_2CH_3)(CH_2CH_3)$ A), 10.3 (s, $N(CH_2CH_3)(CH_2CH_3)$ A), 8.3 (s, $N((CH_2CH_3)_2)$ B). IR: ν N−O 1854.7, 1826.1. HRMS: *m*/*z* 524.0961 (M^+, calcd *m*/*z* 524.0938).

Synthesis of 8 from 7. To an ethereal suspension (3 mL) of **7** (20 mg, 0.048 mmol) at −34 °C was added a solution of iPrONa (7.55 mg, 0.092 mmol) in THF (2 mL) at the same temperature, resulting in an immediate color change to green. The reaction mixture was stirred for 40 min at the same temperature, 24 h at ambient temperature, and 3 days under reflux. The reaction was filtered, and the solvent was removed under vacuum to give pure **8** in 29% yield. Crystals suitable for X-ray analysis were obtained by slow evaporation of ethanol from a concentrated ethanol solution of **8**. $^{31}P\{^1H\}$ NMR (C_6D_6): 56.6 (s). ^1H NMR (C_6D_6): 7.75 (d, 1H, $^3J_{HH}$ = 7.2 Hz, Py-H3), 7.32 (d, 1H, $^3J_{HH}$ = 7.2 Hz, Py-H5), 7.21 (t, 1H, J_{HH} = 7.2 Hz, Py-H4), 3.80 (s, 2H, $PyCH_2N$), 3.27 (d, $^2J_{HP}$ = 11 Hz, 2H, PCH_2Py), 2.47 (q, 4H, $^3J_{HH}$ = 7 Hz, CH_3CH_2N), 1.08 (d, 18H, $^3J_{PH}$ = 13 Hz, $P(C(CH_3)_3)_2$), 0.98 (t, 6H, $^3J_{HH}$ = 6.9 Hz, NCH_2CH_3). $^{13}C\{^1H\}$ NMR (C_6D_6): 160.2 (s, Py-C6), 154.4 (d, $^2J_{CP}$ = 6 Hz, Py-C2) 136.0 (s, Py-C4), 123.6 (s, Py-C5), 120.3 (s, Py-C3), 59.8 (s, $PyCH_2N$), 47.3 (s, NCH_2CH_3), 35.9 (d, $^1J_{CP}$ = 58 Hz, $P(C(CH_3)_3)_2$), 32.9 (s, $^1J_{CP}$ = 58 Hz, PCH_2Py), 26.6 (bs, $P(C(CH_3)_3)_2$), 12.1 (s, NCH_2CH_3). IR: ν N−O 1928.3, 1679 cm^{-1}. HRMS: *m*/*z* 454.1571 (M^+, calcd *m*/*z* 454.1561).

Synthesis of 8 from $Ru(NO)Cl_3{\cdot}2H_2O$. To a solution of $Ru(NO)Cl_3{\cdot}2H_2O$ (27.2 mg, 0.1 mmol) and PNN (32.2 mg, 0.1 mmol) in ethanol (3 mL) was added Et_3N (30.3 mg, 0.3 mmol) under nitrogen atmosphere, and the reaction mixture was stirred under reflux for 19 h. The reaction mixture was allowed to cool to ambient temperature, and the solvent was removed under vacuum. The residue was extracted with 5 mL of THF and filtered, the solvent was removed under vacuum, and the residue was extracted with 1 mL of benzene. Evaporation of the solvent under vacuum gave pure **8** in 18% yield.

dx.doi.org/10.1021/ic401780p | *Inorg. Chem.* 2013, 52, 11469−11479

Table 8. Experimental Data Regarding X-ray Diffraction[a]

	4	5·BF_4	6	8	9
formula	$C_{23}H_{43}Cl_2N_2OP_2Ru$ + $C_{32}H_{12}BF_{24}$ + $C_4H_{10}O$	$C_{23}H_{43}N_2OP_2Ru$ + BF_4	$C_{23}H_{42}N_2OP_2Ru$	$C_{19}H_{35}ClN_3OPRu$	$2C_{18}H_{33}Cl_2N_3OPRu$ + $C_{15}NORu$ + $2CH_2Cl_2$
diffractometer	Bruker APEX - II	Bruker APEX - II	Nonius	Bruker APEX - II	Nonius
cryst description	green plate	orange blue prism	brown prism	red needle	orange prism
cryst size, mm^3	0.50 × 0.30 × 0.10	0.25 × 0.20 × 0.18	0.08x 0.05 × 0.05	0.35 × 0.13 × 0.11	0.45 × 0.15 × 0.08
fw, g mol^{-1}	1534.85	613.41	525.60	488.99	1499.01
space group	$P2_1/c$	$P\bar{1}$	*Pbca*	$P3_121$	$P\bar{1}$
cryst syst	monoclinic	triclinic	orthorhombic	trigonal	triclinic
a, Å	13.7611(5)	8.0668(5)	11.908(2)	14.945(2)	8.30100(10)
b, Å	23.5911(7)	12.3986(7)	15.530(3)		10.90700(10)
c, Å	20.3726(6)	15.5505(8)	28.001(6)	20.484(4)	16.9480(2)
α, deg		108.203(3)			92.6710(10)
β, deg	97.092(2)	102.593(3)			95.3230(10)
γ, deg		92.010(3)			106.7980(10)
cell vol., $Å^3$	6563.1(4)	1432.98(14)	5178.3(18)	3962.3(15)	1458.30(3)
Z	4	2	8	6	1
density(calcd, g cm^{-3})	1.553	1.422	1.348	1.230	1.707
μ, mm^{-1}	0.480	0.703	0.745	0.766	1.459
no. of reflns	121 182	25 268	42 864	33 334	26 236
no. of unique reflns	25 096	5327	6401	5530	6650
Θ_{max}	33.29	25.50	28.28	26.73	27.48
R_{int}	0.0528	0.0498	0.0431	0.0620	0.0326
no. of params (restraints)	1016(48)	368(35)	274(0)	238(0)	310(0)
final *R* for data with $I > 2\sigma(I)$	0.0531	0.0485	0.0490	0.0483	0.0332
final *R* for all data	0.0982	0.0745	0.0740	0.0640	0.0410
goodness of fit	1.024	1.068	1.072	0.871	1.070

[a]Crystals were coated in Paratone oil and mounted on a fiber loop.

Synthesis of 9. To a solution of $Ru(NO)Cl_3·2H_2O$ (136.5 mg, 0.5 mmol) in ethanol (7 mL) was added PN^2N (154 mg, 0.5 mmol) under nitrogen atmosphere, and the mixture was stirred for 1.5 h at room temperature. Solvent was removed under vacuum, and the residue was extracted with 100 mL of CH_2Cl_2 and filtered. Solvent was removed under vacuum, and the residue was washed with CH_2Cl_2 (2 mL) to give pure **9** in 62% yield. Crystals suitable for X-ray analysis were obtained by slow evaporation of a concentrated CH_2Cl_2 solution of **9**. Single crystals of **9** used for X-ray analysis were obtained with $RuCl_5NO^{2-}$ as counteranion. $^{31}P\{^1H\}$ NMR (CD_2Cl_2): 94.3 (s). ^1H NMR (CD_2Cl_2): 8.40 (d, 1H, $^3J_{HH}$ = 7.5 Hz, Py-H3), 8.06 (t, 1H, J_{HH} = 7.5 Hz, Py-H4), 7.70 (d, 1H, $^3J_{HH}$ = 7.5 Hz, Py-H5), 5.03 (dd, $^2J_{HH}$ = 17.1 Hz, $^2J_{HP}$ = 10.2 Hz, 1H, PC*H*HPy), 4.29 (dd, $^2J_{HH}$ = 17.1 Hz, $^2J_{HP}$ = 10.2 Hz, 1H, PC*H*HPy), 3.65 (m, 1H, PyC*H*HCH$_2$N), 3.43 (m, 1H, PyC*H*HCH$_2$N), 3.04 (d, 3H, $^3J_{HP}$ = 2 Hz, NCH_3), 2.96 (m, 1H, PyCH$_2$C*H*HN), 2.84 (m, 4H, PyCH$_2$C*H*HN and NCH_3), 1.67 (d, 9H, $^3J_{PH}$ = 15.5 Hz, P(C(CH_3)$_3$)$_2$), 1.37 (d, 9H, $^3J_{PH}$ = 13 Hz, P(C(CH_3)$_3$)$_2$). $^1H\{^{31}P\}$ NMR (CD_2Cl_2): 8.40 (d, 1H, $^3J_{HH}$ = 7.5 Hz, Py-H3), 8.06 (t, 1H, J_{HH} = 7.5 Hz, Py-H4), 7.70 (d, 1H, $^3J_{HH}$ = 7.5 Hz, Py-H5), 5.09 (d, $^2J_{HH}$ = 17.1 Hz, 1H, NC*H*HPy), 4.34 (d, $^2J_{HH}$ = 17.1 Hz, 1H, PC*H*HPy), 3.65 (m, 1H, PyC*H*HCH$_2$N), 3.51 (m, 1H, PyC*H*HCH$_2$N), 3.10 (s, 3H, NCH_3), 3.04−2.94 (m, 4H, PyCH$_2$C*H*HN and PyCH$_2$C*H*HN), 2.84 (s, 3H, NCH_3), 1.67 (bd, 9H, $^3J_{PH}$ = 7 Hz, P(C(CH_3)$_3$)$_2$), 1.39 (bs, 9H, P(C(CH_3)$_3$)$_2$). $^{13}C\{^1H\}$ NMR (CD_2Cl_2): 164.4 (s, Py-C2) 160.3 (s, Py-C6), 142.3 (s, Py-C4), 126.6 (s, Py-C5), 126.1 (d, $^3J_{CP}$ = 9 Hz, Py-C3), 58.5 (s, PyCH$_2$CH$_2$N), 49.6 (s, NCH_3), 49.2 (s, NCH_3), 40.9 (d, $^1J_{CP}$ = 5.6 Hz, P(C(CH$_3$)$_3$)$_2$), 40.8 (d, $^1J_{CP}$ = 5.6 Hz, P(C(CH$_3$)$_3$)$_2$), 36.0 (s, PyCH$_2$CH$_2$N), 35.7 (d, $^1J_{CP}$ = 24 Hz, PCH$_2$Py), 30.4 (bs, P(C(CH_3)$_3$)$_2$), 30.1 (bs, P(C(CH_3)$_3$)$_2$). IR: *ν* N−O 1854.7 cm^{-1}. HRMS: *m*/*z* 510.0792 (M^+, calcd *m*/*z* 510.0782).

Synthesis of 10 from 9. A THF solution (2 mL) of iPrONa (20 mg, 0.0367 mmol) was added to a THF solution (3 mL) of **9** (20 mg, 0.0367 mmol) at −34 °C. The reaction mixture was stirred for 1 h at the same temperature, 24 h at ambient temperature, and 65 °C overnight. The reaction mixture was allowed to cool to ambient temperature and then filtered, and the solvent was removed under vacuum to yield pure **10** in 30% yield. $^{31}P\{^1H\}$ NMR (C_6D_6): 56.9 (s). ^1H NMR (C_6D_6): 7.68 (d, 1H, $^3J_{HH}$ = 7.8 Hz, Py-H3), 7.12 (t, 1H, J_{HH} = 7.8 Hz, Py-H4), 6.69 (d, 1H, $^3J_{HH}$ = 7.8 Hz, Py-H5), 3.24 (d, $^2J_{HP}$ = 10.8 Hz, 2H, PCH_2Py), 2.94 (t, 2H, $^3J_{HH}$ = 7.3 Hz, PyCH_2CH$_2$N), 2.72 (t, 2H, $^3J_{HH}$ = 7.3 Hz, PyCH$_2$CH_2N), 2.15 (s, 6H, NCH_3), 1.15 (d, 18H, $^3J_{PH}$ = 12.9 Hz, P(C(CH_3)$_3$)$_2$). $^{13}C\{^1H\}$ NMR (C_6D_6): 159.7 (s, Py-C2) 154.9 (s, Py-C6), 135.7 (s, Py-C4), 123.0 (s, Py-C5), 120.5 (s, Py-C3), 67.5 (s, PyCH$_2$CH$_2$N), 45.5 (s, NCH_3), 45.2 (s, NCH_3), 36.1 (s, P(C(CH$_3$)$_3$)$_2$), 35.7 (s, P(C(CH$_3$)$_3$)$_2$), 33.1 (m, PCH$_2$Py), 29.9 (s, PyCH$_2$CH$_2$N), 27.2 (bs, P(C(CH$_3$)$_3$)$_2$). IR: *ν* N−O 1589.1 cm^{-1}. MS: *m*/*z* 475.13 (M^+, calcd *m*/*z* 475.11). HRMS: *m*/*z* 440.1418 ($(M - Cl^-)^+$, calcd *m*/*z* 440.1405).

Synthesis of 10 from $Ru(NO)Cl_3·2H_2O$. To a solution of $Ru(NO)Cl_3·2H_2O$ (136.5 mg, 0.5 mmol) and PN^2N (154 mg, 0.5 mmol) in ethanol (15 mL) was added Et_3N (0.506 g, 5 mmol) under nitrogen atmosphere. The reaction mixture was stirred under reflux for 3 h. Solvent was removed under vacuum and remained under vacuum for 2 h. THF (15 mL) was added, and the reaction mixture was stirred under argon overnight (to allow hydrogen escape). Solvent was removed under vacuum, and crude **10** was extracted once with ether (15 mL) and twice with benzene (15 mL). The ethereal and benzene solutions were combined, filtered, and evaporated to yield pure **10** in 87% yield.

Catalytic Dehydrogenation of Alcohols. A solution of **6** (13.1 mg, 0.025 mmol) and *n*-hexanol (255.4 mg, 5 mmol) was stirred at reflux under argon atmosphere in an open system for 12 h to yield pure hexyl hexanoate in quantitative yield.

Catalytic Dehydrogenative Coupling of Hexanol to Ethyl Acetate under Air. A solution of **6** (13.1 mg, 0.025 mmol), *n*-hexanol (255.4 mg, 5 mmol), and *m*-xylene (1.5 mL) was stirred at reflux under air in an open system overnight to yield hexyl hexanoate

dx.doi.org/10.1021/ic401780p | Inorg. Chem. 2013, 52, 11469−11479

in quantitative yield. According to GC-MS a trace of hexanal was also formed (>0.5%).

Computational Details. All calculations were carried out using Gaussian 03 Revision E.01[38] and Gaussian 09 Revision C.01.[39] The former was locally modified with the MNGFM patch;[40] this patch from the University of Minnesota adds the Minnesota-06 family of DFT exchange-correlation functionals to the commercial version. Two members of the Minnesota-06 family of DFT functional[41] were used: M06, a meta-hybrid functional containing 27% HF exchange,[42] and M06-L, its local (nonhybrid) variant.[43]

With these functionals, the SDB-cc-pVDZ basis set-RECP (relativistic effective core potential) combination was used. This combines the Dunning cc-pVDZ basis set[44] on the main group elements and the Stuttgart–Dresden basis set-RECP[45] on the transition metals with an added *f*-type polarization exponent taken as the geometric average of the two *f* exponents given in the appendix of ref 46.

In order to improve the efficiency of the calculations, density fitting basis sets (DFBS) were employed during calculation of the Coulomb interaction. The automatic DFBS generation algorithm as implemented in Gaussian was employed.[47,48]

The accuracy of the DFT methods was improved by adding the second-generation empirical dispersion correction recommended by Grimme.[49,50] The s_6 empirical scaling factors, unique for each DFT functional, have been determined for M06-L and M06 to be 0.20 and 0.25, respectively.[51]

Bulk solvent effects were approximated by single-point energy calculations using a polarizable continuum model (PCM),[52−55] specifically the integral equation formalism model (IEF-PCM)[52,53,56,57] with ethanol as the solvent as in the experiments. In the PCM model, the United Atom Topological Model was used with the atomic radii from the UFF force field with explicit spheres on the hydrogen atoms.

Geometries were optimized using the default pruned (75,302) grid, while the "ultrafine" (i.e., a pruned (99,590)) grid was used for energy and solvation calculations, especially essential for calculations with the M06 family of functionals.[58]

Charges presented are atomic polarization tensor (APT) charges[59] taken from the frequency calculations.

X-ray Crystal Structure Determination of Complexes 4, 5·BF_4, 6, 8, and 9. Crystals were placed in Paratone oil (Hampton Research), mounted in a MiTeGen loop, and flash frozen in a nitrogen stream at 100 K. Data were collected on either a Bruker APEX-II KappaCCD diffractometer or a Nonius KappaCCD diffractometer mounted on a FR590 generator. Both are equipped with a sealed tube with Mo Kα radiation (λ = 0.71073 Å) MiraCol optics and a graphite monochromator. Data were processed and scaled using the Bruker Apex2 SAINT suite or Denzo, respectively. Structures were solved using direct methods with SHELXS-97 and refined with SHELXL-97 using full-matrix least-squares refinement based on F^2. CIF files are included as separate files. X-ray data are summarized in Table 8.

■ ASSOCIATED CONTENT

Ⓢ Supporting Information

Copies of NMR spectra of the new complexes and CIF files giving X-ray data for **4**, **5**·BF_4, **6**, **8**, and **9** are included. This material is available free of charge via the Internet at http://pubs.acs.org.

■ AUTHOR INFORMATION

Corresponding Author

*E-mail: david.milstein@weizmann.ac.il.

Notes

The authors declare no competing financial interest.

■ ACKNOWLEDGMENTS

This research was supported by the European Research Council under the FP7 framework (ERC No 246837). D.M. is the holder of the Israel Matz Professorial Chair of Organic Chemistry.

■ REFERENCES

(1) Zhang, J.; Gandelman, M.; Shimon, L. J. W.; Rozenberg, H.; Milstein, D. *Organometallics* **2004**, *23*, 4026−4033.
(2) Zhang, J.; Leitus, G.; Ben-David, Y.; Milstein, D. *J. Am. Chem. Soc.* **2005**, *127*, 10840.
(3) Zhang, J.; Gandelman, M.; Shimon, L. J. W.; Milstein, D. *Dalton Trans.* **2007**, 107−113.
(4) Gargir, M.; Ben-David, Y.; Leitus, G.; Diskin-Posner, Y.; Shimon, L. J. W.; Milstein, D. *Organometallics* **2012**, *31*, 6207−6214.
(5) Fogler, E.; Balaraman, E.; Ben-David, Y.; Leitus, G.; Shimon, L. J. W.; Milstein, D. *Organometallics* **2011**, *30*, 3826−3833 and references within.
(6) Zhang, J.; Leitus, G.; Ben-David, Y.; Milstein, D. *Angew. Chem., Int. Ed.* **2006**, *45*, 1113−1115.
(7) Balaraman, E.; Fogler, E.; Milstein, D. *Chem. Commun.* **2012**, *48*, 1111−1113.
(8) Gunanathan, C.; Ben-David, Y.; Milstein, D. *Science* **2007**, *317*, 790−792.
(9) Gnanaprakasam, B.; Zhang, J.; Milstein, D. *Angew. Chem., Int. Ed.* **2010**, *49*, 1468−1471.
(10) Srimani, D.; Feller, M.; Ben-David, Y.; Milstein, D. *Chem. Commun.* **2012**, *48*, 11853−11855.
(11) Gunanathan, C.; Shimon, L. J. W.; Milstein, D. *J. Am. Chem. Soc.* **2009**, *131*, 3146−3147.
(12) Kossoy, E.; Diskin-Posner, Y.; Leitus, G.; Milstein, D. *Adv. Synth. Catal.* **2012**, *354*, 497−504.
(13) Van der Boom, M. E.; Milstein, D. *Chem. Rev.* **2003**, *103*, 1759−1792 and references within.
(14) Gunanathan, C.; Milstein, D. *Angew. Chem., Int. Ed.* **2008**, *47*, 8661−8664.
(15) Gnanaprakasam, B.; Ben-David, Y.; Milstein, D. *Adv. Synth. Catal.* **2010**, *352*, 3169−3173.
(16) Gnanaprakasam, B.; Balaraman, E.; Ben-David, Y.; Milstein, D. *Angew. Chem.* **2011**, *123*, 12448−12452.
(17) Balaraman, E.; Ben-David, Y.; Milstein, D. *Angew. Chem.* **2011**, *123*, 11906−11909.
(18) Balaraman, E.; Gunanathan, C.; Zhang, J.; S himon, L. J. W.; Milstein, D. *Nat Chem* **2011**, *3*, 609−614.
(19) Langer, R.; Leitus, G.; Ben-David, Y.; Milstein, D. *Angew. Chem., Int. Ed.* **2011**, *50*, 2120−2124.
(20) Gnanaprakasam, B.; Milstein, D. *J. Am. Chem. Soc.* **2011**, *133*, 1682−1685.
(21) Gunanathan, C.; Milstein, D. In *Bifunctional Molecular Catalysis*; Ikariya, T., Shibasaki, M., Eds.; Springer: Berlin, Heidelberg, 2011; Vol. *37*, pp 55−84 and references within.
(22) Langer, R.; Diskin-Posner, Y.; Leitus, G.; Shimon, L. J. W.; Ben-David, Y.; Milstein, D. *Angew. Chem., Int. Ed.* **2011**, *50*, 9948−9952.
(23) Balaraman, E.; Gnanaprakasam, B.; Shimon, L. J. W.; Milstein, D. *J. Am. Chem. Soc.* **2010**, *132*, 16756−16758.
(24) Balaraman, E.; Ben-David, Y.; Milstein, D. *Angew. Chem., Int. Ed.* **2011**, *50*, 11702−11705.
(25) Richter-Addo, G. B., Legzdins, P. *Metal Nitrosyls*; Oxford University Press: New York, 1992.
(26) Faller, J. W.; Lambert, C.; Mazzieri, M. R. *J. Organomet. Chem.* **1990**, *383*, 161−177.
(27) Crabtree, R. H. *The Organometallic Chemistry of the Transition Metals*; 4th ed.; John Wiley & Sons, Inc.: Hoboken, NJ, 2005.
(28) Collman, J. P.; Hegedus, L. S.; Finke, R. G. *Principles and Applications of Organotransition Metal Chemistry*; University Science Books: Mill Valley, CA, 1987 and references within.
(29) Collman, J. P.; Farnham, P.; Dolcetti, G. *J. Am. Chem. Soc.* **1971**, *93*, 1788−1790.

(30) Verma, A.; Hirsch, D. J.; Glatt, C. E.; Ronnett, G. V.; Snyder, S. H. *Science* **1993**, *259*, 381−384.
(31) Enemark, J. H.; Feltham, R. D. *Coord. Chem. Rev.* **1974**, *13*, 339−406.
(32) Jiang, Y.; Schirmer, B.; Blacque, O.; Fox, T.; Grimme, S.; Berke, H. *J. Am. Chem. Soc.* **2013**, *135*, 4088−4102.
(33) Hayton, T. W.; Legzdins, P.; Sharp, W. B. *Chem. Rev.* **2002**, *102*, 935−992.
(34) Nagao, H.; Enomoto, K.; Wakabayashi, Y.; Komiya, G.; Hirano, T.; Oi, T. *Inorg. Chem.* **2007**, *46*, 1431−1439.
(35) Walstrom, A.; Pink, M.; Fan, H.; Tomaszewski, J.; Caulton, K. G. *Inorg. Chem.* **2007**, *46*, 7704−7706 and references within.
(36) Watson, L. A.; Pink, M.; Caulton, K. G. *J. Mol. Catal. A: Chem.* **2004**, *224*, 51−59.
(37) Ahmad, N.; Levison, J. J.; Robinson, S. D.; Uttlky, M. F.; Wonchoba, E. R.; Parshall, G. W. Complexes of Ruthenium, Osmium, Rhodium, and Iridium Containing Hydride Carbonyl, or Nitrosyl Ligands. In *Inorganic Synthisis*; John Wiley & Sons, Inc.: Hoboken, NJ, 2007; Vol *15*, pp 45−64.
(38) Frisch, M. J.; Trucks, G. W.; Schlegel, H. B.; Scuseria, G. E.; Robb, M. A.; Cheeseman, J. R.; Montgomery, J. A., Jr.; Vreven, T.; Kudin, K. N.; Burant, J. C.; Millam, J. M.; Iyengar, S. S.; Tomasi, J.; Barone, V.; Mennucci, B.; Cossi, M.; Scalmani, G.; Rega, N.; Petersson, G. A.; Nakatsuji, H.; Hada, M.; Ehara, M.; Toyota, K.; Fukuda, R.; Hasegawa, J.; Ishida, M.; Nakajima, T.; Honda, Y.; Kitao, O.; Nakai, H.; Klene, M.; Li, X.; Knox, J. E.; Hratchian, H. P.; Cross, J. B.; Bakken, V.; Adamo, C.; Jaramillo, J.; Gomperts, R.; Stratmann, R. E.; Yazyev, O.; Austin, A. J.; Cammi, R.; Pomelli, C.; Ochterski, J. W.; Ayala, P. Y.; Morokuma, K.; Voth, G. A.; Salvador, P.; Dannenberg, J. J.; Zakrzewski, V. G.; Dapprich, S.; Daniels, A. D.; Strain, M. C.; Farkas, O.; Malick, D. K.; Rabuck, A. D.; Raghavachari, K.; Foresman, J. B.; Ortiz, J. V.; Cui, Q.; Baboul, A. G.; Clifford, S.; Cioslowski, J.; Stefanov, B. B.; Liu, G.; Liashenko, A.; Piskorz, P.; Komaromi, I.; Martin, R. L.; Fox, D. J.; Keith, T.; Al-Laham, M. A.; Peng, C. Y.; Nanayakkara, A.; Challacombe, M.; Gill, P. M. W.; Johnson, B.; Chen, W.; Wong, M. W.; Gonzalez, C.; Pople, J. A. *Gaussian 03*, Revision E.01; Gaussian, Inc.: Wallingford, CT, 2004.
(39) Frisch, M. J.; Trucks, G. W.; Schlegel, H. B.; Scuseria, G. E.; Robb, M. A.; Cheeseman, J. R.; Scalmani, G.; Barone, V.; Mennucci, B.; Petersson, G. A.; Nakatsuji, H.; Caricato, M.; Li, X.; Hratchian, H. P.; Izmaylov, A. F.; Bloino, J.; Zheng, G.; Sonnenberg, J. L.; Hada, M.; Ehara, M.; Toyota, K.; Fukuda, R.; Hasegawa, J.; Ishida, M.; Nakajima, T.; Honda, Y.; Kitao, O.; Nakai, H.; Vreven, T.; Montgomery, J. A., Jr.; Peralta, J. E.; Ogliaro, F.; Bearpark, M.; Heyd, J. J.; Brothers, E.; Kudin, K. N.; Staroverov, V. N.; Kobayashi, R.; Normand, J.; Raghavachari, K.; Rendell, A.; Burant, J. C.; Iyengar, S. S.; Tomasi, J.; Cossi, M.; Rega, N.; Millam, J. M.; Klene, M.; Knox, J. E.; Cross, J. B.; Bakken, V.; Adamo, C.; Jaramillo, J.; Gomperts, R.; Stratmann, R. E.; Yazyev, O.; Austin, A. J.; Cammi, R.; Pomelli, C.; Ochterski, J. W.; Martin, R. L.; Morokuma, K.; Zakrzewski, V. G.; Voth, G. A.; Salvador, P.; Dannenberg, J. J.; Dapprich, S.; Daniels, A. D.; Farkas, O.; Foresman, J. B.; Ortiz, J. V.; Cioslowski, J.; Fox, D. J. *Gaussian 09*, Revision C.01; Gaussian, Inc.: Wallingford, CT, 2009.
(40) Zhao, Y.; Truhlar, D. G. with assistance from Iron, M. A.; Martin, J. M. L. *Minnesota Gaussian Functional Module*, version 3.1; University of Minnesota: Minneapolis, MN, 2008.
(41) Zhao, Y.; Truhlar, D. G. *Acc. Chem. Res.* **2008**, *41*, 157−167.
(42) Zhao, Y.; Truhlar, D. G. *Theor. Chem. Acc.* **2008**, *120*, 215−241.
(43) Zhao, Y.; Truhlar, D. G. *J. Chem. Phys.* **2006**, *125*, 194101.
(44) Dunning, T. H., Jr. *J. Chem. Phys.* **1989**, *90*, 1007−1023.
(45) Dolg, M. In *Modern Methods and Algorithms of Quantum Chemistry*; Grotendorst, J., Ed.; John von Neumann Institute for Computing: Jülich, Germany, 2000; Vol. *3*, pp 507−540.
(46) Martin, J. M. L.; Sundermann, A. *J. Chem. Phys.* **2001**, *114*, 3408−3420.
(47) Dunlap, B. I. *J. Chem. Phys.* **1983**, *78*, 3140−3142.
(48) Dunlap, B. I. *J. Mol. Struct. (THEOCHEM)* **2000**, *529*, 37−40.
(49) Schwabe, T.; Grimme, S. *Phys. Chem. Chem. Phys.* **2007**, *9*, 3397−3406.
(50) Schwabe, T.; Grimme, S. *Acc. Chem. Res.* **2008**, *41*, 569−579.
(51) Karton, A.; Tarnopolsky, A.; Lamère, J.-F.; Schatz, G. C.; Martin, J. M. L. *J. Phys. Chem. A* **2008**, *112*, 12868−12886.
(52) Mennucci, B.; Tomasi, J. *J. Chem. Phys.* **1997**, *106*, 5151−5158.
(53) Cancès, E.; Mennucci, B.; Tomasi, J. *J. Chem. Phys.* **1997**, *107*, 3032−3041.
(54) Cossi, M.; Barone, V.; Mennucci, B.; Tomasi, J. *Chem. Phys. Lett.* **1998**, *286*, 253−260.
(55) Cossi, M.; Scalmani, G.; Rega, N.; Barone, V. *J. Chem. Phys.* **2002**, *117*, 43−54.
(56) Mennucci, B.; Cancès, E.; Tomasi, J. *J. Phys. Chem. B* **1997**, *101*, 10506−10517.
(57) Tomasi, J.; Mennucci, B.; Cancès, E. *J. Mol. Struct. (THEOCHEM)* **1999**, *464*, 211−226.
(58) Wheeler, S. E.; Houk, K. N. *J. Chem. Theory Comput.* **2010**, *6*, 395−404.
(59) Cioslowski, J. *J. Am. Chem. Soc.* **1989**, *111*, 8333−8336.